Nanoscale Res Lett (2009) 4:359–363
DOI 10.1007/s11671-009-9253-6

NANO EXPRESS

Characterization and Optical Properties of the Single Crystalline SnS Nanowire Arrays

G. H. Yue · L. S. Wang · X. Wang · Y. Z. Chen · D. L. Peng

Received: 28 October 2008 / Accepted: 8 January 2009 / Published online: 23 January 2009

Abstract The SnS nanowire arrays have been successfully synthesized by the template-assisted pulsed electrochemical deposition in the porous anodized aluminum oxide template. The investigation results showed that the as-synthesized nanowires are single crystalline structures and they have a highly preferential orientation. The ordered SnS nanowire arrays are uniform with a diameter of 50 nm and a length up to several tens of micrometers. The synthesized SnS nanowires exhibit strong absorption in visible and near-infrared spectral region and the direct energy gap E_g of SnS nanowires is 1.59 eV.

Keywords SnS nanowires · Pulse electrodeposition · Optical properties

Introduction

Semiconductor nanostructures have been attracting worldwide attention due to their exceptional electrical, optical, and magnetic properties, and their potential applications in nanoscale electronics, photonics, and functional materials as well [1–3]. Among them, tin sulfide (SnS) has sparked intensive interest for its semiconducting and optical properties. SnS, as one of the important IV–VI group semiconductors, exhibits both the *p*- and *n*-type conduction [4], has an energy band gap of about 1.3 eV [5]. Normally, SnS is composed of double layers of tightly bound Sn–S atoms and the bonding between layers are extremely weak Van der Vaals forces, which has an orthorhombic structure [6]. Additionally, SnS has the advantage of its constituent elements being abundant in nature and not posing any health and environmental hazards. Therefore, SnS has a big potential to be used as solar absorber in a thin film solar cell and near-infrared detector [4, 5], as photovoltaic materials [7], and as a holographic recording medium [8]. Therefore, single crystalline SnS nanowires reported in this paper are expected to offer enhanced properties. Therefore, it is important to investigate practical synthesis routes for novel SnS nanostructures, especially in single crystalline.

Crystalline tin sulfides have been prepared by a variety of methods, such as direct vapor transport method [9], stoichiometric composition technique [10], physical vapor transport method [11], and Bridgman–Stockbarger technique [12]. In recent years, thin films of SnS have been investigated widely due to their applications in photovoltaic and photoelectrochemical solar cells. SnS thin films have been prepared by spray pyrolytic deposition [13], electrochemical deposition [4, 5], chemical vapor deposition [14, 15], and chemical bath deposition [16]. To our knowledge, preparation of novel wire-like SnS nanostructures has been reported sparsely. Panda et al. [17] has reported surfactant-assisted synthesis of SnS nanowires grown on tin foils and SnS nanorods were reported by Biswas et al. [18]. We had used the anodic aluminum oxide (AAO) template synthesized from some metal sulfide nanowire arrays [19, 20] and in this paper, we have presented single crystalline SnS nanowires prepared by template-assisted electrochemical deposition.

G. H. Yue · L. S. Wang · X. Wang · Y. Z. Chen · D. L. Peng (✉)
Department of Materials Science and Engineering, Research Center of Materials Design and Applications, Xiamen University, Xiamen 361005, People's Republic of China
e-mail: dlpeng@xmu.edu.cn

G. H. Yue
e-mail: yuegh@126.com

Experimental

The highly ordered porous AAO films were prepared by anodizing an aluminum foil (99.999%) in an acid solution using a two-step anodizing process, which could be seen in the Refs. [19–22].

A three-electrode cell was used for pulse electrochemical deposition: a saturated calomel electrode (SCE) as the reference electrode, an AAO template with aluminum substrate as the working electrode (cathode), and a platinum sheet as the contrary electrode (anode). The deposition area was about 1×2 cm^2. An aqueous bath containing 30 mM $SnCl_2$ and 100 mM $Na_2S_2O_3$ was used. The pH value of the solution was around 1.8 before deposition. The temperature of the solution was kept at 10 °C. The potential applied to the cathode was pulsed-form, its "on" potential V_{on} was 10 V and "off" potential V_{off} was 0 V, both "on" time and "off" time were 10 s in all the voltage conditions. More details of the experiment can be seen in the Refs. [4, 20, 21]. Deposition period was 5 min. After deposition experiment, the deposited sample was washed softly in pure water, and naturally dried in air. All the chemicals used were analytical grade reagents and the water used was deionized distilled water.

The phase purity of as-synthesized product was examined by X-ray diffraction (XRD) using Rigaku Rint-2000 diffractometer with monochromatized CuK_α radiation ($\lambda = 0.15405$ nm). The nano/microstructure of the SnS product was further observed by transmission electron microscope (TEM) and field-emission scanning electron microscope (FESEM) with an energy dispersive spectrometer (EDS) analysis attachment, which were performed on a Hitachi Model H-800 (200 kV) and a field-emission microscope (S-4800, 15 kV), respectively. The high resolution transmission electron microscope (HRTEM) image and the corresponding selected area electron diffraction (SAED) pattern were taken by a JEOL-2010 TEM with an accelerating voltage of 200 kV. UV–VIS–NIR absorption spectra were measured at room temperature with a Cary 5000 UV–VIS–NIR spectrometer.

Results and Discussion

The typical XRD pattern of the sample which etched for 5 h is shown in Fig. 1. The peaks at about 30.44°, 32.06°, 54.42°, and 64.14° were assigned to (101), (040), (240), and (212) diffraction of orthorhombic SnS, respectively. All the peaks can be indexed to orthorhombic SnS with lattice constants: a = 4.34 Å, b = 11.14 Å, and c = 3.96 Å, which is in good agreement with the values from the standard card (JCPDS No. 39-0354). The strong and sharp diffraction peaks indicate that the product is well

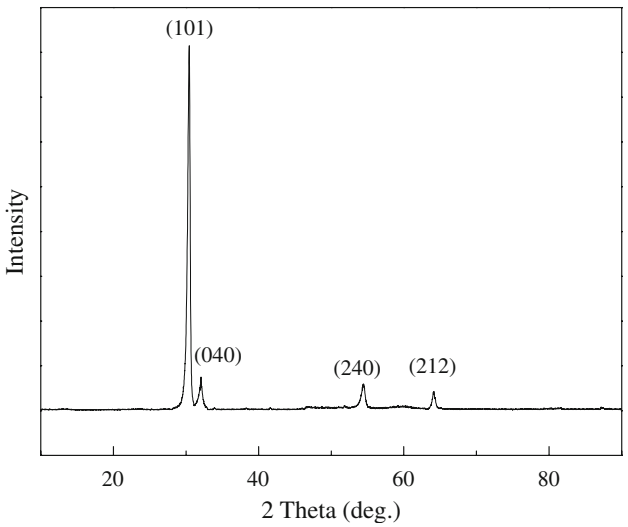

Fig. 1 XRD patterns of the SnS nanowire arrays after etching time of 5 h

crystallized. It can be seen that the major peak (101) is strongly dominating other peaks indicating the preferred orientation. The sharp and narrow (101) peaks indicate that the nanowires are highly crystalline and consist of only a single compositional phase. XRD analysis detected no impurities such as SnO_2 and SnS_2.

Figure 2a shows a typical SEM micrograph of the AAO template, anodized using 0.3 M H_2SO_4 electrolyte at 0 °C and a voltage of 20 V. It was found that the nanopores of the AAO template are uniform and highly ordered with average diameters of 50 ± 4 nm and the interpore distance is about 30 nm. In addition, the varied diameters and lengths of nanopores can be obtained by adjusting the varied acid, anodizing time, and anodizing temperature. Figure 2b–d show the SEM images of SnS nanowires grown in AAO template. These photographs indicate that the nanowires are uniformly distributed, highly ordered, and parallel to each other. Few microscopic defects are found in these wires. Figure 2b, c is a planform, from which we can find several clusters of nanowires. The clusters may result from the situation that the nanowires do not cover by the framework of AAO template but stand free incompletely. When the alumina on the top of AAO template is dissolved away, the nanowires that embedded in the template are released gradually and incline to agglutinate together. It is conceivable that the surface energy of these nanowires causes this interesting phenomenon. Figure 2b also shows that SnS nanowires are abundant, uniform, and highly ordered in the large area. Figure 2d reveals a cross-section where the alumina matrix of the AAO template has been partially dissolved away. It can be seen that the nanowires deposited inside the nanochannel of the AAO template are parallel, tidily aligned,

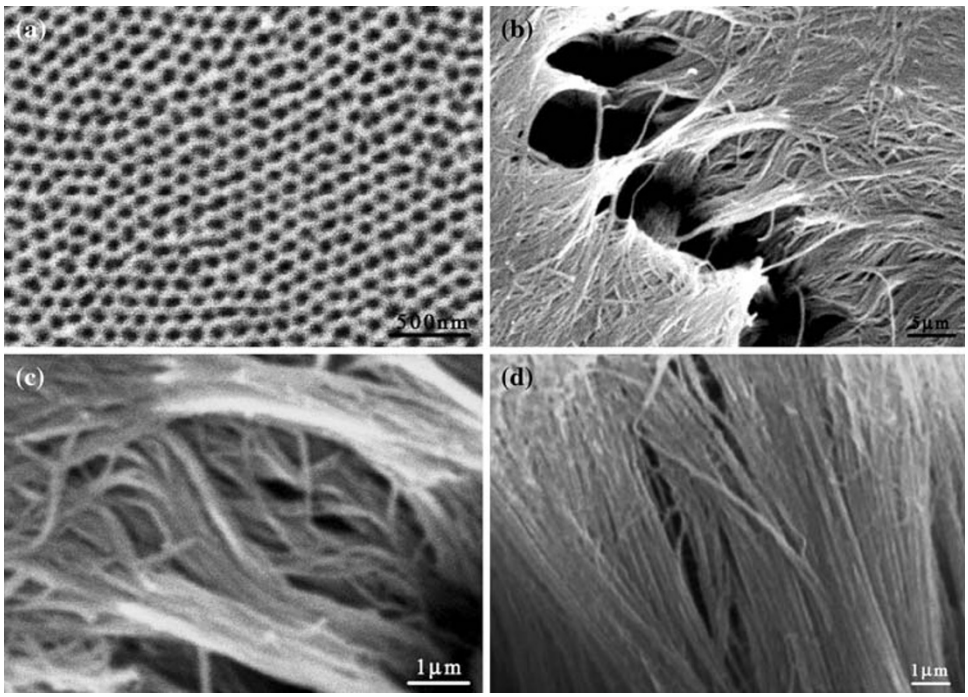

Fig. 2 SEM images of AAO template and SnS nanowire arrays. **a** Typical SEM image of AAO template. **b** and **c** The top view in a low magnification. **d** SEM image of a typical cross-section

and uniformly distributed. It is correlative to that the AAO template had an array of densely parallel nanoholes arranged in a hexagonal form. From these figures it can be estimated that the length of the nanowires is about several tens of micrometers. It corresponds with the thickness of the AAO template which we used.

TEM images of SnS nanowires formed within the AAO template are shown in Fig. 3a, b. Figure 3a shows that the SnS nanowires cross and overlap with each other, and Fig. 3b shows that the diameter of the SnS nanowires is about 50 nm. It's diameter is approximately equal to that of the nanochannels of the employed AAO template. These nanowires are uniformly distributed, which indicates that the alumina matrix is dissolved completely. The nanostructure of the SnS nanowires was further investigated with SAED. The SAED pattern (Fig. 3c) taken from a single nanowire, indicates that the SnS nanowires are a good single crystalline. The HRTEM image of a single SnS

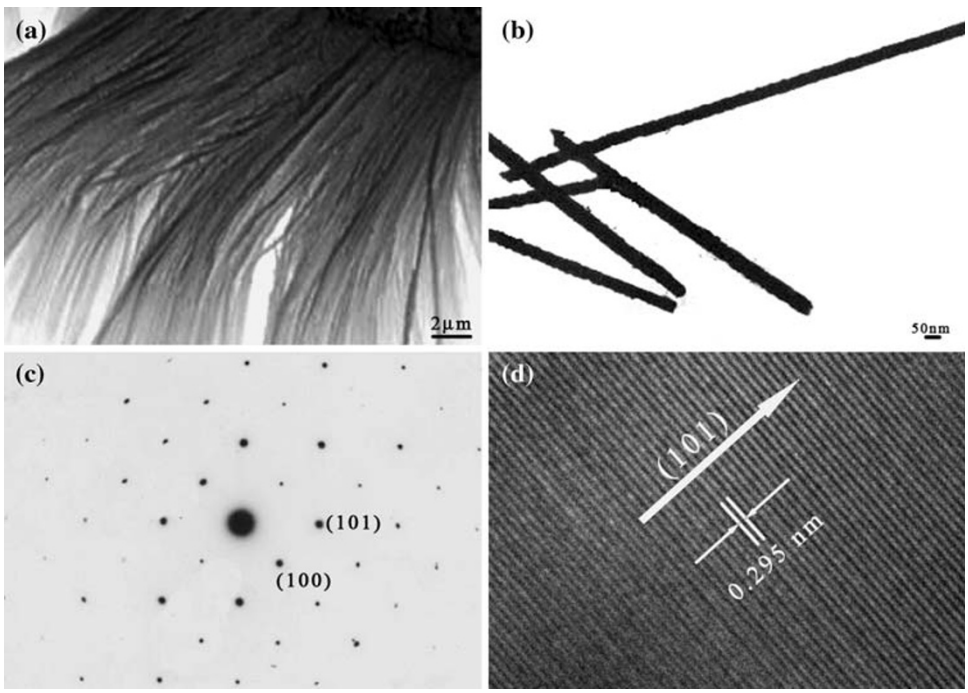

Fig. 3 TEM images of AAO template and SnS nanowire arrays. **a** The sample was etched for 10 h. **b** The SnS nanowires with a diameter of about 50 nm. **c** The SAED pattern taken from the nanowires in (**b**). **d** The HRTEM image of the SnS nanowires in (**b**)

nanowire is given in Fig. 3d. Seen from this image, the lattice fringes of the SnS are clear and uniform, and additionally it confirmed that these single crystalline SnS nanowires are of high quality. The measured spacing of the crystallographic planes shown in Fig. 3d is 0.295 nm, corresponding to the value of (101) planes of the orthorhombic SnS nanowires.

Energy dispersive spectrometer (EDS) analysis reveals that the product is composed of stannum and sulfur, and the ratio of the S atom and Sn atom is 1:0.985, which just accords with the stoichiometric ratio of SnS.

The representative optical absorption spectrum of the SnS nanowires synthesized by template-assisted electrochemical deposition is shown in Fig. 4a. This figure indicated that the SnS nanowires have high absorption in the range of ultraviolet, and the absorption coefficient is above the 70%. The absorption reduces rapidly with the increase in the wavelength, and the absorption is very small or becomes zero when the wavelength is above 800 nm. The absorption coefficient α, of SnS nanowires, was calculated from the average absorption index (A) as $\alpha = 4\pi A/\lambda$ [23]. The spectral behavior of absorption coefficient as a function of energy, $h\nu$, is shown in Fig. 4b. SnS nanowires have high absorption coefficient ($>10^5$ cm^{-1}) in the wavelength range from 400 to 800 nm.

To determine the energy band gap, E_g, and the type of optical transition responsible for this intense optical absorption, and the absorption spectrum was analyzed using the equation for the near-edge absorption [4, 5].

$$(\alpha h\nu)^n = A(h\nu - E_g)$$

where, A is a constant and n characterizes the transition process. We can see $n = 2$ and 2/3 for direct allowed and forbidden transitions, respectively, and $n = 1/2$ and 1/3 for indirect allowed and forbidden transitions, respectively.

Figure 5 shows curves of $(\alpha h\nu)^2$ versus $h\nu$ of the SnS nanowires. The curve has a good straight line fit with higher energy range above the absorption edge, indicating a direct optical transition near the absorption edge. Based on Fig. 5, the direct energy gap E_g of the sample has been calculated as 1.59 eV, which is higher than the literature value of SnS bulk or films [4, 5, 13, 16]. The increased band gap values of SnS nanowires which was compared to the bulk material, do not manifest quantum size effects. However, the estimated average single crystal nanowire diameter was 50 nm. The absence of size quantization effects may be attributed to the very small Bohr radius for the SnS. And it is well-known that Bohr radius of SnS should be smaller than 7 nm. The nanowires diameter is far greater than the Bohr radius and it can be suggested that the increased band gap values do not manifest quantum size effects [24, 25]. The energy band gap at 1.59 eV detected in our previous study may be attributed to the surface effect of the carriers in the semiconductor nanowires. The lattice distortion inducing a smaller lattice constant or surface lattice defects will lead to a size dependent enlargement of

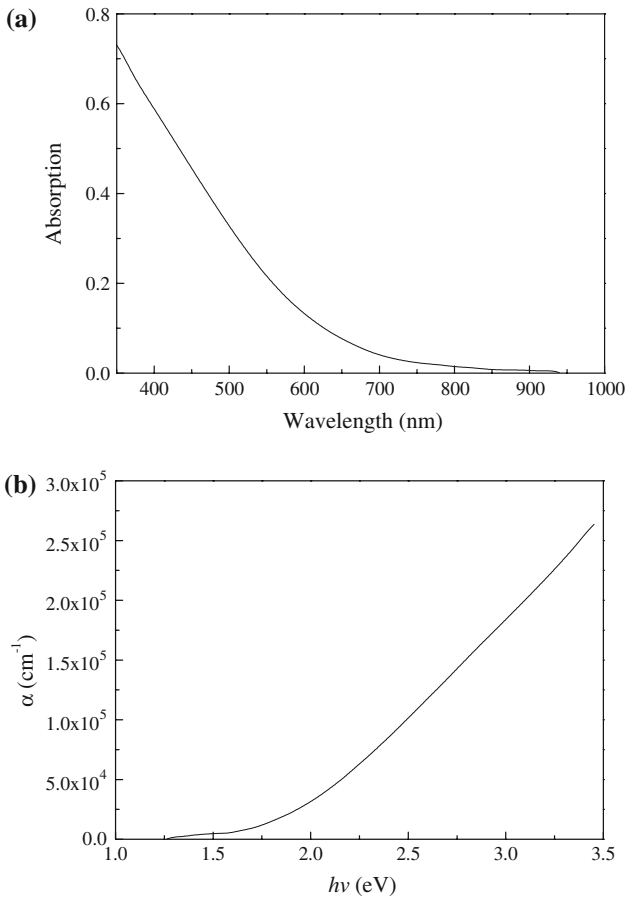

Fig. 4 Optical properties of SnS nanowires: **a** is the optical absorption spectrum and **b** is the dependence of absorption coefficient on photon energy

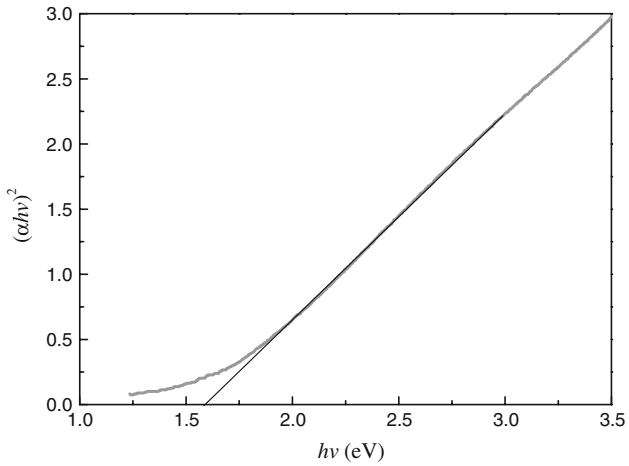

Fig. 5 The curves of $(\alpha h\nu)^2$ vs. $h\nu$ for the SnS nanowires

the band gap, which results in a blue shift in the absorbance onset, as observed in this work.

Conclusion

The low-toxicity SnS nanowire arrays have been successfully synthesized using the template-assisted pulsed electrochemical deposition in the AAO template. The XRD pattern indicates that the nanowires are composed of SnS phase and have a highly preferential (101) orientation. The sample obtained in our experiment forms a stable orthorhombic superstructure. The TEM images show that the diameter of the SnS nanowires is about 50 nm and length up to several tens of micrometers. The SAED shows that the product is single crystalline structure. EDS result indicates that the ratio of S atom and Sn atom in our samples is 1:0.985, which just accords with the stoichiometric ratio of SnS. The synthesized SnS nanowires exhibit strong absorption in the visible and near-infrared spectral region. The direct energy gap E_g of the SnS nanowires has been calculated as 1.59 eV, and this experimental optical band gap value is the evidence for the quantum confinement of the SnS nanowires.

Acknowledgments This work was partially supported by the National Outstanding Youth Science Foundation of China (No. 50825101), and the National Natural Science Foundation of China (No. 50671087). The correspondence author (D. L. Peng) acknowledges the Minjiang Chair Professorship Program released by Fujian Province of P.R. China for financial support.

References

1. X. Duan, Y. Huang, R. Agarwal, C.M. Lieber, Nature **421**, 241 (2003). doi:10.1038/nature01353
2. G.H. Yue, P.X. Yan, D. Yan et al., Appl. Phys. A **84**, 409 (2006). doi:10.1007/s00339-006-3643-8
3. M.S. Fuhrer, J. Nygard, L. Shih et al., Science **288**, 494 (2000). doi:10.1126/science.288.5465.494
4. G.H. Yue, D.L. Peng et al., J. Alloy Compd. (2008). doi:10.1016/j.jallcom.2008.01.047
5. G.H. Yue, W. Wang et al., J. Alloy Compd. (2008). doi:10.1016/j.jallcom.2008.06.105
6. A. Ghazali, Z. Zainal, M.Z. Hussein, A. Kassim, Sol. Energy Mater. Sol. Cells **55**, 237 (1998). doi:10.1016/S0927-0248(98)00106-8
7. J.P. Singh, R.K. Bedi, Thin Solid Films **199**, 9 (1991)
8. M. Radot, Rev. Phys. Appl. (Paris) **18**, 345 (1977)
9. S.K. Arora, D.H. Patel, M.K. Agarwal, J. Cryst. Growth **131**, 268 (1993). doi:10.1016/0022-0248(93)90422-S
10. E.P. Trifonova, I.Y. Yanchev, V.B. Stoyanova et al., Mater. Res. Bull. **31**, 919 (1996). doi:10.1016/S0025-5408(96)00083-9
11. J. George, C.K. Valsalakumari, K.S. Joseph, J. Appl. Phys. **54**, 5347 (1983). doi:10.1063/1.332711
12. M.J. Powel, J. Phys. C: Solid State Phys. **10**, 2967 (1977). doi:10.1088/0022-3719/10/15/029
13. B. Thangaraju, P. Kaliannan, J. Phys. D: Appl. Phys. (Berl) **33**, 1054 (2000)
14. A. Ortiz, J.C. Alonso, M. Garcia, J. Toriz, Semicond. Sci. Technol. **11**, 243 (1996). doi:10.1088/0268-1242/11/2/017
15. L.S. Price, I.P. Parkin, M.N. Field et al., J. Mater. Chem. **10**, 527 (2000). doi:10.1039/a907939d
16. A. Tanusevski, Semicond. Sci. Technol. **18**, 501 (2003). doi:10.1088/0268-1242/18/6/318
17. S.K. Panda, A. Datta, A. Dev, S. Gorai, S. Chaudhuri, Cryst. Growth Des. **6**, 2179 (2006). doi:10.1021/cg0602156
18. S. Biswas, S. Kar, S. Chaudhuri, Appl. Surf. Sci. **253**, 9259 (2007). doi:10.1016/j.apsusc.2007.05.053
19. G.H. Yue, P.X. Yan, J.Z. Liu, X.Y. Fan, R.F. Zhuo, Appl. Phys. Lett. **87**, 262505 (2005). doi:10.1063/1.2158521
20. G.H. Yue, P.X. Yan, L.S. Wang et al., Nanotechnology **19**, 195706 (2008). doi:10.1088/0957-4484/19/19/195706
21. G.H. Yue, P.X. Yan, X.Y. Fan et al., J. Appl. Phys. **100**, 124313 (2006). doi:10.1063/1.2403243
22. G.H. Yue, P.X. Yan, X.Y. Fan et al., Electrochem. Solid-State Lett. **10**, D29 (2007). doi:10.1149/1.2430564
23. M.M. El-Nahass, H.M. Zeyada, M.S. Aziz, N.A. El-Ghamaz, Opt. Mater. **20**, 159 (2002). doi:10.1016/S0925-3467(02)00030-7
24. H. Tang, G.Y. Xu, L.Q. Weng, L.J. Pan, L. Wang, Acta Mater. **52**, 1489 (2004). doi:10.1016/j.actamat.2003.11.030
25. T. Takagahara, Phys. Rev. B **47**, 4569 (1993). doi:10.1103/PhysRevB.47.4569